Chemical Engineering Journal 414 (2021) 128821

Contents lists available at ScienceDirect

Chemical Engineering Journal

journal homepage: www.elsevier.com/locate/cej

Short communication

Methane to ethylene by pulsed compression

Y. Slotboom [a,*], S. Roosjen [a], A. Kronberg [b], M. Glushenkov [b], S.R.A. Kersten [a,*]

[a] Sustainable Process Technology, Faculty of Science and Technology, University of Twente, PO Box 217, 7500 AE Enschede, The Netherlands
[b] Encontech B.V., P.O. Box 217, 7500 AE, Enschede, The Netherlands

ARTICLE INFO

Keywords:
Methane
Thermal coupling
Ethylene
Compression
Non-oxidative
Non-catalytic

ABSTRACT

Pulsed compression is introduced for the conversion of methane, by pyrolysis, into ethylene. At the point of maximal compression temperatures of 900 to 1620 K were reached, while the initial and final temperature of the gas did not exceed 523 K. By the use of a free piston reactor concept pressures of up to 460 bar were measured with nitrogen as a diluting gas. From 1100 K onwards methane conversion was measured. By increasing the temperature, the mechanism of pyrolytic methane conversion, being subsequent production of ethane, ethylene, acetylene, …, benzene, and ultimately tar/soot, was clearly observed. Without hydrogen in the feed, the attainable operating window (C2-selectivity vs. methane conversion) observed was similar to other catalytic oxidative and non-oxidative coupling processes. With hydrogen, in a first attempt to optimize the product yield, 24% C2-yield (62% ethylene selectivity, 93% C2-selectivity) at 26% conversion was reached without producing observable soot. It is worthwhile to explore pulsed compression further because it does not require a catalyst and therefore, does not deactivate over time and it operates at low reactor temperature.

For many decades, the direct coupling of methane to olefins has been studied [1–3]. This process is considered to be attractive because: (1) methane is abundantly available and production is increasing, e.g. by recent fracturing techniques [4], (2) it poses a more cost-effective and environmentally friendly alternative to the energy intensive naphtha steam crackers [2,5], (3) it provides the possibility of local and small-scale production of olefins [6], e.g. from methane that would have been flared otherwise [7,8]. The impact of replacing naphtha by methane can be substantial, since products like ethylene and propylene are bulk chemicals with respectively a demand of 150 and 100 megatonnes/year [9].

There are two direct routes from methane towards olefins being investigated: oxidative coupling of methane (OCM) and non-oxidative coupling of methane (NCM, investigated in this work). To date, both routes require catalysis and many catalytic systems for OCM and NCM have been investigated [1–4,10,11]. Plasma techniques (NCM) can convert methane non-catalytically. However, acetylene is the main product [12] and thus catalysis is required to hydrogenate to ethylene [13].

Typically, C_2-yields of OCM are between 10 and 20% with peaks to 30% [3,14]. Most of the research was carried out at laboratory-scale and a small number of pilot-plants have been in operation [15]. A drawback of using OCM is the downgrading of a part of the feedstock (i.e. producing CO_2), thus having a low carbon efficiency. The challenge lies in selectivity control, since any (oxygenated) hydrocarbon is more reactive than methane itself [1]. Other challenges reported are the heating of a gaseous feed to the temperatures of around 1073–1173 K, the difficulty in heat management of the exothermic reaction and the stability of the catalyst [14]. High energy consumption of the separation train in combination with low C_2-yields (<25%) make the process still far from competitive on both capital expenditures and operational expenditures compared to the conventional naphtha steam cracking [5,16]. The drawbacks of OCM increased the interest in NCM [1,17–19]. NCM is essentially the pyrolysis of methane. The main challenge of methane pyrolysis for the production of olefins is to achieve high conversion and prevent soot formation, as no oxygen is there to prevent that [17,19]. At temperatures of 973–1173 K reported C_2-yields (ethane, ethylene and acetylene) were typically limited to 5% (Pt–Bi or Ni–P catalyst) [20,21]. Somewhat higher temperatures (≈ 1373 K) resulted in yields of around 23% of ethylene using a single iron site catalyst [22]. At the Institut Français du Pétrole pilot scale research was conducted [23]. However, the severe conditions and catalyst deactivation in combination with low yields have limited NCM from commercialization [4,17].

In this work we introduce a low temperature (<573 K) non-oxidative, non-catalytic and non-plasma method to convert methane to ethylene and other valuable products. We report here our first observations, without a complete understanding of the underlying phenomena yet, to make the findings available to the community

* Corresponding authors.
E-mail addresses: y.slotboom@utwente.nl (Y. Slotboom), s.r.a.kersten@utwente.nl (S.R.A. Kersten).

https://doi.org/10.1016/j.cej.2021.128821
Received 10 November 2020; Received in revised form 25 January 2021; Accepted 30 January 2021
Available online 8 February 2021

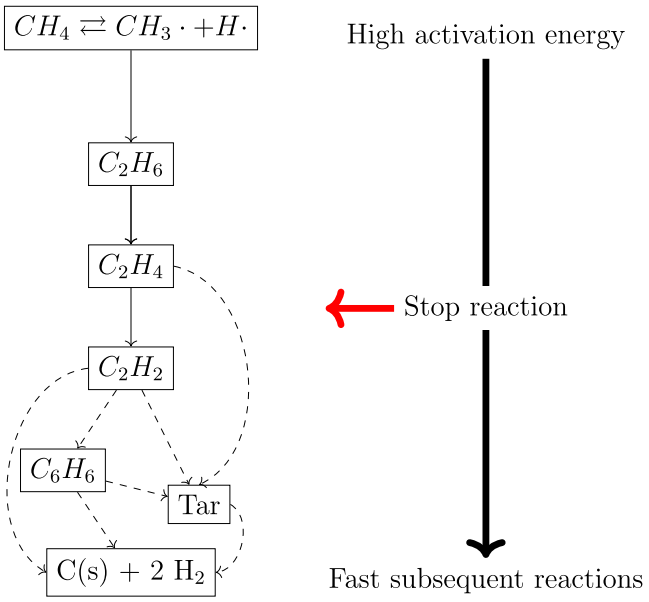

Fig. 1. Simplified reaction path of methane pyrolysis [17,24–27].

for further exploration of its opportunities. The method is based on pulsed compression of methane. Pulsed stands for very fast compression and subsequent decompression. The high temperatures reached by the compression enable the pyrolysis of methane.

The difficulty of thermal is that the first step has a very high activation energy between 419 and 452 kJ mol^{-1} [30] and thus requires a high temperature, but once that is overcome methane can react all the way down to soot, as displayed in Fig. 1. Hence, the desired products are intermediates in the reaction chain. The only way to produce ethylene is to stop it in the middle by quenching with unconventional speeds. Or in other words: only allow for a very short reaction time at high temperature.

The pulsed compression reactor (PCR) can achieve the required conditions of fast heating to high temperatures and rapid quenching [31,32]. The first description of a compression reactor dates back to 1926 and was invented by M. Brutzkus [33], who proposed it for cracking hydrocarbons. More recent versions of that are rapid compression machines. Recently the potential of a rapid compression machine is discussed in detail [34–36]. The PCR used in this study is shown in Fig. 2. It is a compression reactor with a free piston, which was designed for research purposes at the University of Twente [32]. The PCR has many similarities with a ballistic compressor, of which the first research on methane pyrolysis was conducted in 1958 by P.A. Longwell [37]. The difference is the ability to perform shots repeatedly after each other, without the need for re-assembly of the set-up.

The PCR has the feature of being able to reach high temperatures of up to 1300 K as in Fig. 2 in 8 ms, reaching heating rates of $1 \cdot 10^5$ K/s, see Supporting Information for the calculation. More importantly, it quenches the reaction products at the same rate during expansion back to atmospheric pressure (see Fig. 2), thereby stopping the reactions towards soot. There are two energy inputs for this system, one is the pre-heating of the gas and the other is the amount of work supplied through the launch gas. The amount of energy needed for methane pyrolysis in the PCR is the endothermic internal energy change of the reaction, the friction losses and heat losses during compression. The heat losses are not quantified at this point, so for this work it is assumed during calculations that the gas is compressed adiabatically. We will report on the energy balance in an upcoming publication.

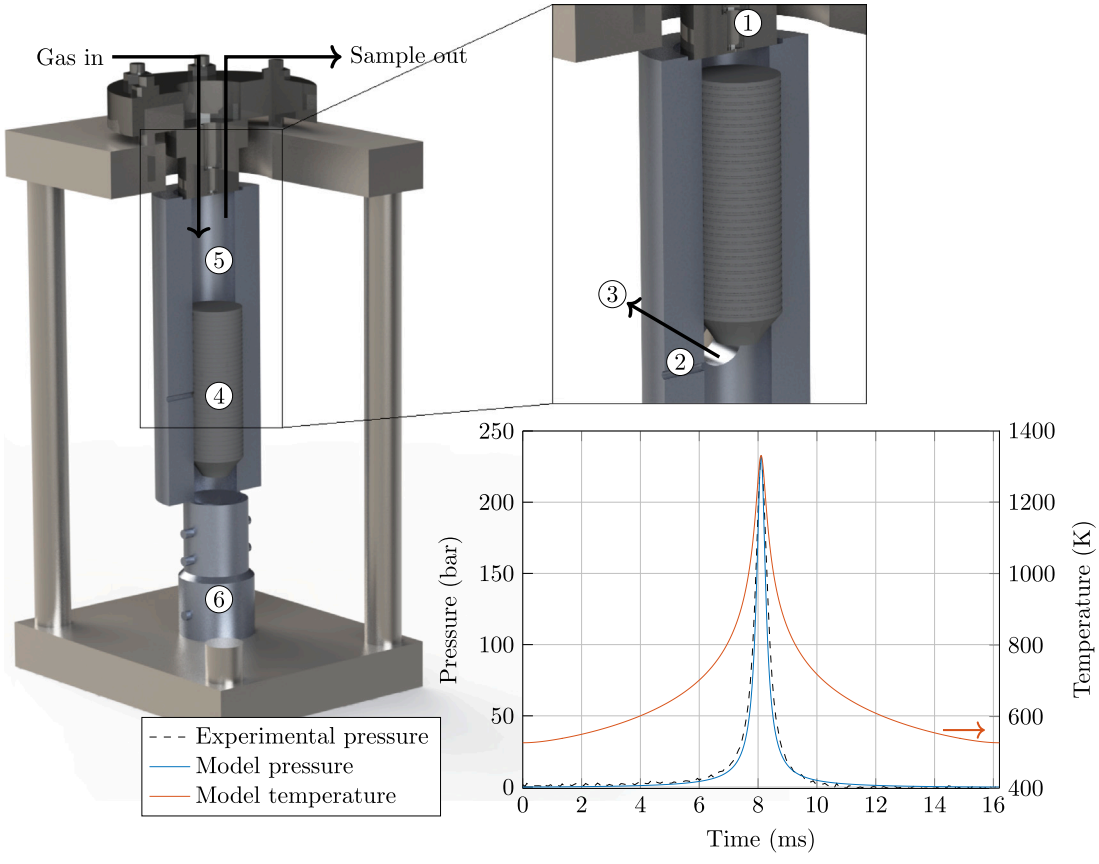

Fig. 2. Schematic representation of the pulsed compression reactor. The reactor is operated batch wise. The figure shows a pressure and temperature curve of a typical pulse. 1. Pressure sensor 2. Laser sensor 3. Launch gas release holes 4. Moveable piston 5. Reactant chamber 6. Launch mechanism.

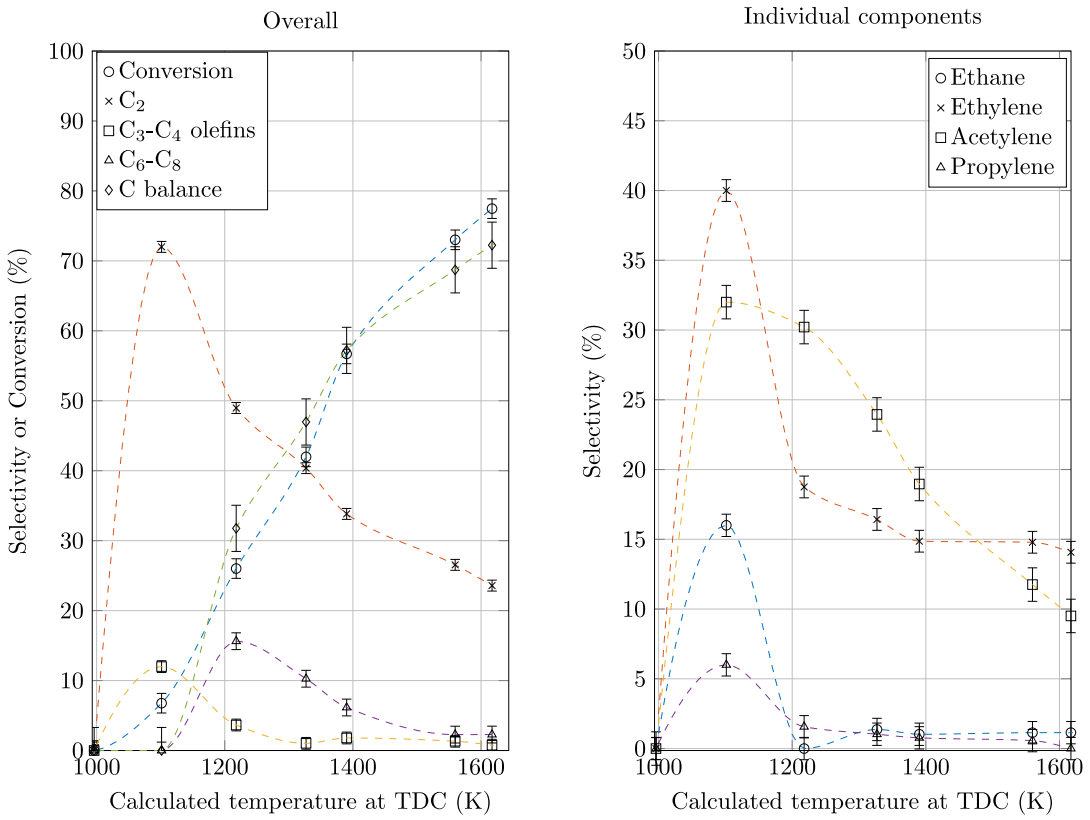

Fig. 3. Single shot results of 8% of methane in argon at an initial reactor temperature of 523 K. Conversion and selectivities are plotted. Lines are for guidance purposes only. A similar graph was obtained for the series in nitrogen, as displayed in the Supporting Information.

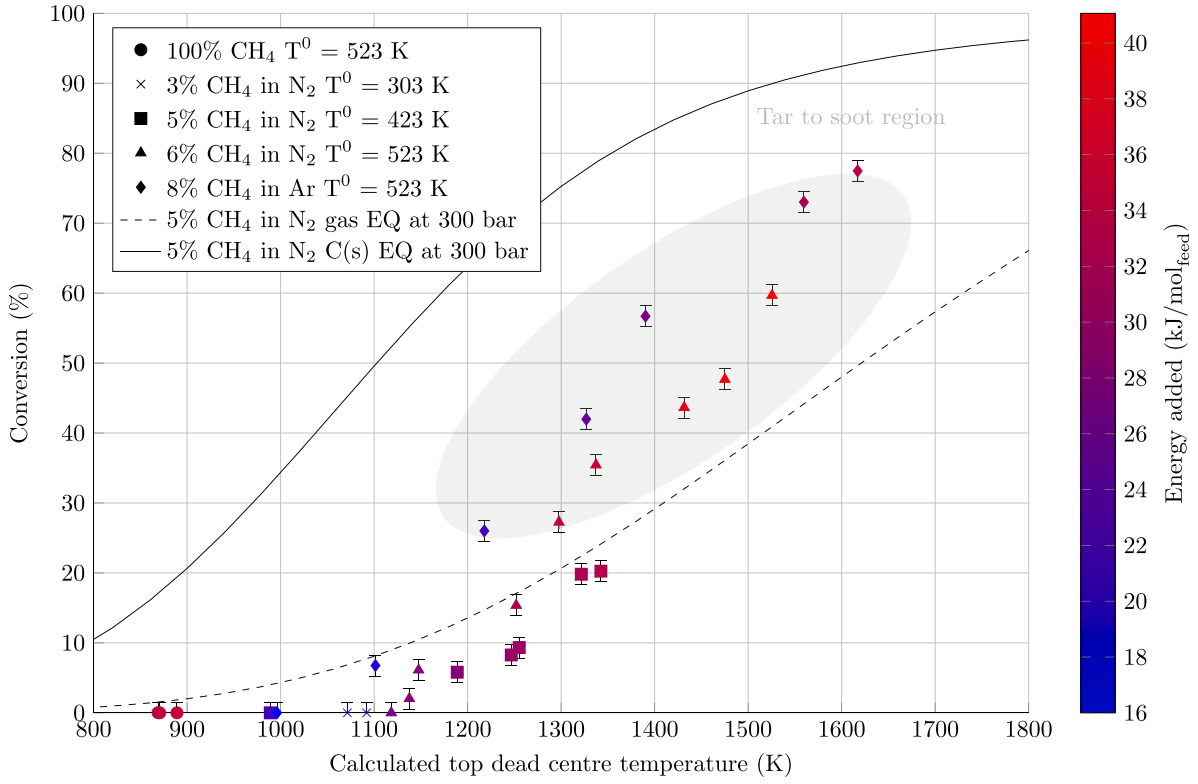

Fig. 4. Single shot results of the pulsed compression reactor (PCR) including equilibrium lines and energy input (calculations and additional EQ lines can be found in the Supporting Information). The TDC temperature is calculated based on the measured pressure curve (Fig. 5), inlet composition and real adiabatic compression relations calculated with the GERG-EoS [28].

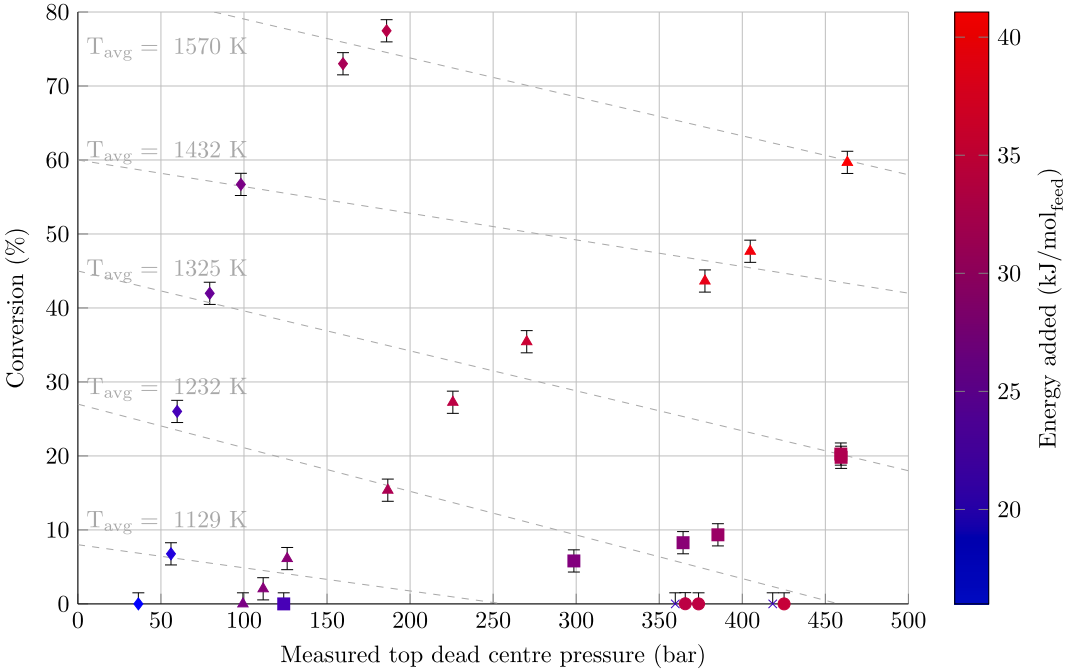

Fig. 5. Single shot results of the pulsed compression reactor (PCR). The shown isotherms are average values of the points adjacent to the lines. The same legend of Fig. 4 applies here. The isotherms do not apply for experimental points with zero conversion.

The piston and cylinder were machined in such a precise manner that a gap of only 10–30 μm exists between piston and stainless steel wall. This creates a sealing and causes the gas to be the lubricant itself, replacing the need for oil. The reactor body was made out of stainless steel. For reducing friction between materials the piston was made out of graphite (Entegris (POCO) ACF-10Q grade) and it weighs 0.869 kg. Pre-heating of the reactor and inlet gas in order to achieve higher compression temperatures and pressures was possible. Tests were done at initial temperatures of 303, 423 and 523 K. The difference between the thermal expansion coefficient of stainless steel and graphite causes the gap to become bigger at elevated temperatures, thus three pistons were machined with different diameters. To perform a compression on a mixture the reactant chamber (nr. 5 in Fig. 2) was filled with a certain feed composition at atmospheric pressure. Then the piston (nr. 4) was launched by releasing a fraction of a 130 ml volume of pressurized nitrogen (nr. 6, up to 140 bar) underneath the piston. Typical launch pressures used were between 50 and 110 bar. To make sure only a single shot is performed most of the launch gas was released through the holes on the side (nr. 3). Release holes in the bottom part (not shown) damp the next bounce of the piston. The position of the piston (either piston is seen or not seen) was measured by a Keyence FS-V31M laser (nr. 2) to determine the time at which the piston first moves. The pressure was measured in the top (nr. 1) by an Optrand D732A8 pressure sensor using a sampling frequency of 150 kHz. The compositions of the mixture were measured before and after a shot using a Varian-450 gas chromatograph (GC). This GC is able to measure a range of permanent gases and identify separate hydrocarbons up to C5. Everything from C6 to C8 cannot be separately identified and is therefore grouped under the name C6–C8. Solid carbonaceous deposits were observed inside the reactor and condensed tar was found in the gas samples. The sum of carbonaceous deposits and the tar is termed soot and/or carbon balance, the amount of which is quantified by calculation. The conversion and selectivities are on carbon basis. The absolute error margin on the conversion is 1.4%, on the C_2 selectivity it is 2.0% and on the C_2 yield it is 0.53%. The complete experimental procedure and calculations can be found in the Supporting Information.

The maximum point which the piston reaches is called the top dead centre (TDC), which is variable for each shot. The TDC temperature was not measured, however it was calculated according to adiabatic compression relations [38] and a reactor model using real gas approximations from the GERG-2008 equation of state [28]. In this calculation the heat of reaction was neglected, because of the uncertainty of the soot composition. It was estimated that by inclusion of the heat of reaction the temperature would be 0–200 K lower in the range between 0 and 78 % conversion (see Supporting information). The fast expansion after reaching TDC causes the reaction time to be as short as < 100 μs (see graph in Fig. 2). The achievable TDC temperature depends on the isentropic exponent of the mixture. As an example: compressing a gas from atmospheric pressure to 100 bar starting at 523 K results in a TDC temperature of 3370 K for pure argon, of 1220 K for pure nitrogen and of 1310 K for 10% (molar basis) methane in argon.

Fig. 3 shows conversion and selectivity versus TDC temperature for an experimental series of 8% methane in argon. At 1100 K, conversion was 8% and the highest selectivity was measured for ethane, ethylene, acetylene and C_2-C_3 olefins. This proves that the PCR is indeed able to start methane decomposition and to quench the reaction path at the desired products. The formation of products observed in the PCR as a function of temperature follows the reaction scheme proposed as in Fig. 1, globally. At first ethane is formed, followed by ethylene, acetylene and propylene. At higher temperatures, soot becomes the main product. Soot was only present when either acetylene or benzene was also measured.

A set of results going from 100% methane to a dilution of only 3% of methane in N_2 and Ar is shown in Figs. 4 and 5. Fig. 5 shows the conversion against the measured pressure at TDC and Fig. 4 shows it against the calculated temperature based on the measured TDC pressure. The 60% conversion point in nitrogen reached a pressure of 460 bar and 1530 K, having a compression ratio of 132.

In Fig. 4 two equilibrium (EQ) lines are plotted (see Supporting Information for calculations): one giving the conversion versus temperature when assuming that only gaseous compounds are present (gas EQ line in Fig. 4), the other assuming that gases are in equilibrium with solid carbon (C(s) EQ line in Fig. 4). These calculations show that there is also a thermodynamic limit to the conversion of methane. When a measurement was positioned in the region between the predicted equilibrium lines with and without solid carbon, the product slate contained intermediate products like polycyclic aromatic hydrocarbons

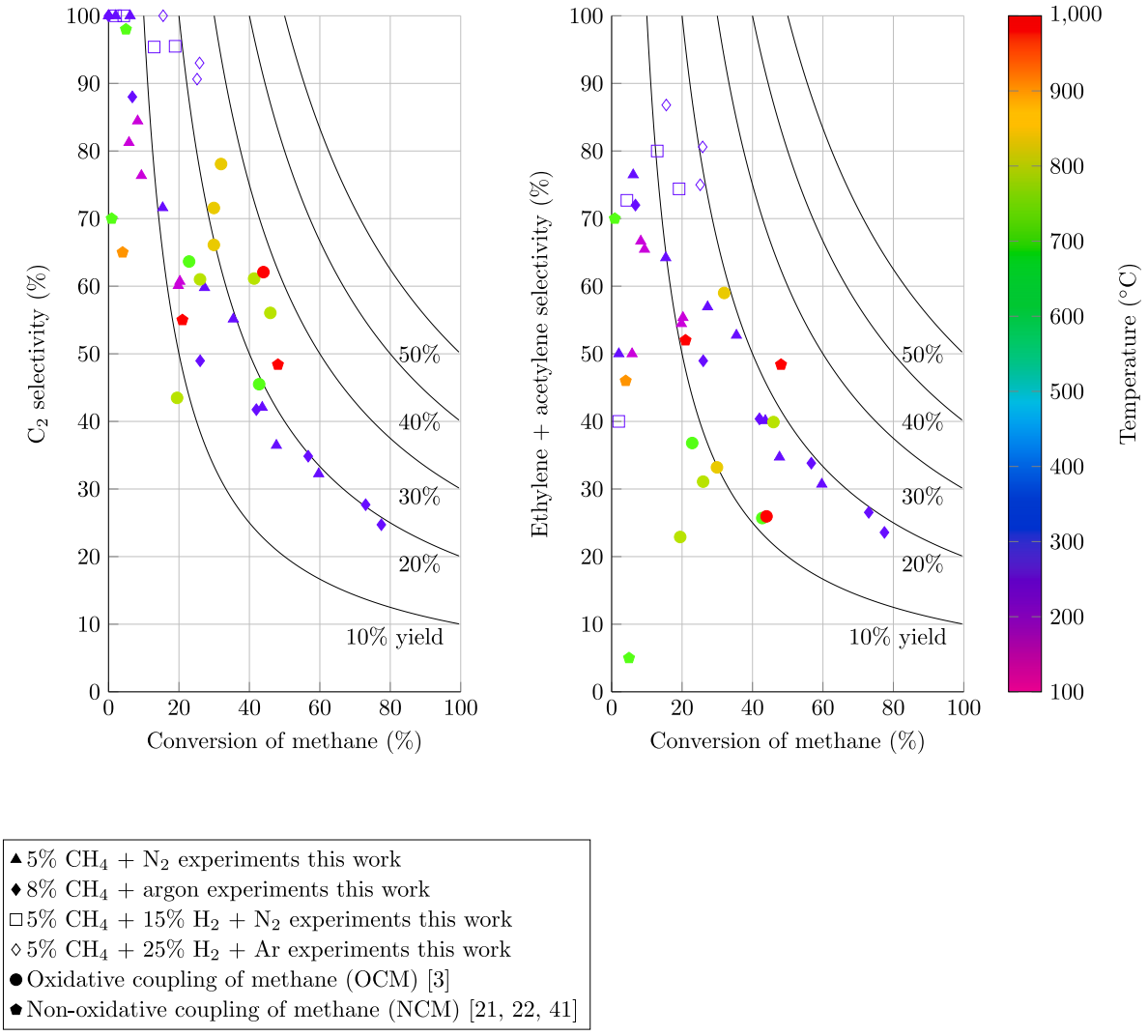

Fig. 6. Comparison of pulsed compression versus OCM [3] and NCM [21,22,29]. Adapted and partly reproduced from Gao et al. [3]. C_2 selectivity includes ethane, ethylene and acetylene.

and/or soot. For an industrial process it is favourable to stay away from tar/soot production. In that case chemical equilibrium will dictate low single pass conversion, e.g. 20% for 5% CH_4 in nitrogen at 1300 K (see Fig. 4).

It is confirmed that the determining factor for the reaction to start is temperature, or in other words the collision of molecules instead of a unimolecular dissociation. The threshold lies between 1100 and 1150 K, only if this temperature or higher is achieved the reactions start. Energy input is not the determining factor. This is most supported by the 100% methane shots where high amounts of energy were put in, but no conversion was observed. While the total energy input was amongst the highest, 900 K is by far too low to start the reaction. The same conclusion can be drawn from experiments at similar energy input around 25 kJ mol^{-1} of feed gas. When this amount of energy was added to 8% CH_4 in argon a conversion of 26% was observed. Adding the same amount of energy to 6% CH_4 in N_2 resulted in no conversion at all. The energy input to the whole feed is defined as the sum of the heating of the gas from 298 K to the initial reactor temperature and the amount of work that was put in, which can be calculated by evaluating the integral of -pdV using a reactor model (for details see Supporting Information). Note, this is not the energy needed for the process, but it is the energy put into a single compression. In a continuous process, this energy minus the reaction heat and the friction losses can be recovered.

For methane concentrations below 10% (volume), the compression temperature can easily reach the required 1150 K (and above). Using nitrogen is only possible in the PCR, because it is able to withstand and keep the high pressure of up to 460 bar that is present at the TDC. A conventional (diesel) combustion engine can reach pressures up to 150 and 180 bar at frequencies between 8 to 35 Hz [39]. Possibly these engines can go higher, but the PCR design at this point already grants the possibility to replace the expensive argon that is used in compression research [34,35,40,41]. A disadvantage of introducing nitrogen is the possibility of the formation of nitrated species. The most unwanted one is hydrogen cyanide. According to equilibrium calculations (See Supporting Information) around 1500 K an amount of 0.2 vol% could be present in the product mixture. However, the likelihood of nitrogen bonds breaking at these temperatures is low, as nitrogen bonds are very strong. This will be investigated and reported on in further publications.

The effect of pressure on the conversion at the same temperature is shown with the isotherms in Fig. 5. Around the TDC temperature of 1325 K the pressure is lower in argon and higher in nitrogen mixtures. Starting from an initial reactor temperature of 423 K results in an even higher pressure in order to obtain the same temperature. This high pressure of 460 bar compared to the 80 bar in argon reduces the conversion by a factor 2. The effect of pressure is quite significant, but the temperature remains the most important factor. The temperature

and pressure are strongly linked. Therefore, inevitably the conversion is limited more in nitrogen mixtures. However, a higher conversion results in a lower selectivity, so the high conversion region is not the preferred operating window. This is shown in the left graph of Fig. 6, which shows the C_2 selectivity (ethane, ethylene and acetylene) plotted against the conversion. Experimental results from this work are compared to OCM [3] and NCM [3,21,22].

The OCM data obtained in the temperature range between 873 and 1073 K follow nearly the same C_2-selectivity-conversion path as the PCR at 423–523 K. The difference is the fact that CO_2 and CO are the remainder of the balance, instead of the soot in the PCR. At high temperatures (>1073 K) combined with the use of a selective catalyst OCM is able to achieve C_2 yields above 20%. Although many of these catalysts still suffer from thermal stability issues [14].

The right graph of Fig. 6 shows that the selectivity and yield towards the unsaturated C_2 components ethylene and acetylene is comparable for OCM, NCM and pulsed compression. The absence of a catalyst in the PCR seems to have no significant effect on selectivities. The main difference is observed in a lower ethane production compared to OCM. Catalytic NCM has similar selectivities, though the challenge still lies in maintaining the activity by preventing coke formation [4,17].

The most interesting experiments from this work are the ones containing hydrogen, as displayed in Fig. 6. In a continuous process hydrogen does not have to be added externally, as it is a reaction product. The best shot with 5% CH_4, 15% H_2 and 80% nitrogen reached a conversion of methane of 19% with a selectivity to ethylene of 63% and a C_2 selectivity of 95%. The remainder of the selectivities are 20% ethane, 11% acetylene, 3% of propylene and 3% of C_6-C_8. It is considered that hydrogen suppresses the initial methyl radical formation and as a result leading to less ethylene consumption and less soot formation [17,42,43]. The combination of the hydrogen addition with the high quenching rate of the PCR results in an interesting operating window with high C_2 selectivities and no soot at a conversion above 15%. This is not necessarily the case, since only adding hydrogen is not sufficient for fully reducing soot formation in this conversion region [23,44].

Experiments in argon (Fig. 6 and more detail in Supporting Information) show that conversion can still be increased while maintaining similar C_2 and ethylene + acetylene selectivities, without the formation of soot. The addition of hydrogen is a variable that can steer towards high selectivity with minimal to no soot formation. More research towards the optimal ratio between hydrogen and carbon can provide a viable operating window for pulsed compression. The wall effects are difficult to quantify, but the conversion over a large time span stays constant (see Supporting Information). The reactor cap is made out of stainless steel and after initial shots it is covered with soot. This soot covered situation was the case for all the experiments presented in this paper and over the course of three months of experimenting the reactor cap was never cleaned. In a continuous situation a layer of soot will be quickly formed, thus our results are representative of that situation. The effect of the soot on the gas phase reactions is difficult to quantify, but based on the measurements discussed in the previous paragraph it is possible to operate without producing additional tar or soot.

A disadvantage of compression is that a high dilution is needed, but at a potential piston reciprocation frequency of 62 Hz and 60% scavenging efficiency (40% of product mixture remains in the reactor chamber) the PCR with the current reactor volume of $0.452{\cdot}10^{-3}$ m^3 with the best shot in nitrogen described previously could theoretically produce 2.7 $mol/m^3_{reactor}/s$ of ethylene plus acetylene (268 $kg/m^3_{reactor}/h$). This is a promising starting point considering that the industrial range lies between 1 and 15 $mol/m^3_{reactor}/s$ [45]. Alternatives techniques like OCM produce 0.5 $mol/m^3_{reactor}/s$ of C2 [46] and plasma reaches 2.1 $mol/m^3_{reactor}/s$ of C2 species [13]. Research on higher methane feed concentrations is ongoing. A major advantage of compression is the absence of a catalyst and the low operating temperature.

Concluding, pulsed compression in the pulsed compression reactor (PCR) has opened up a new possibility for converting methane under non-oxidative and non-catalytic conditions into ethylene with promising conversion and selectivity, worthwhile exploring further.

Declaration of competing interest

The authors declare that they have no known competing financial interests or personal relationships that could have appeared to influence the work reported in this paper.

Acknowledgements

We thank Benno Knaken, Johan Agterhorst and Ronald Borst for their skilled support in getting this set-up operational. We also thank Erna Fränzel-Luiten for her support with the analysis. The machining companies Ten Heggeler and Vossebelt are acknowledged for their precision skills that make the PCR work. Furthermore we thank the project partners ISPT, Dow Benelux B.V. and Shell Global Solutions International B.V. for their support and contribution. This work has received co-funding with subsidy from the Topsector Energy by the Ministry of Economic Affairs and Climate Policy in the Netherlands (project number TEEI118005).

Appendix A. Supplementary data

Supplementary material related to this article can be found online at https://doi.org/10.1016/j.cej.2021.128821.

References

[1] P. Schwach, X. Pan, X. Bao, Direct conversion of methane to value-added chemicals over heterogeneous catalysts: Challenges and prospects, Chem. Rev. 117 (13) (2017) 8497–8520, http://dx.doi.org/10.1021/acs.chemrev.6b00715.
[2] Y. Chen, X. Mu, X. Luo, K. Shi, G. Yang, T. Wu, Catalytic conversion of methane at low temperatures: A critical review, Energy Technol. (2019) http://dx.doi.org/10.1002/ente.201900750.
[3] Y. Gao, L. Neal, D. Ding, W. Wu, C. Baroi, A.M. Gaffney, F. Li, Recent advances in intensified ethylene production - A review, ACS Catal. 9 (9) (2019) 8592–8621, http://dx.doi.org/10.1021/acscatal.9b02922.
[4] P. Tang, Q. Zhu, Z. Wu, D. Ma, Methane activation: the past and future, Energy Environ. Sci. 7 (8) (2014) 2580–2591, http://dx.doi.org/10.1039/C4EE00604F.
[5] V. Spallina, I.C. Velarde, J.A.M. Jimenez, H.R. Godini, F. Gallucci, M. Van Sint Annaland, Techno-economic assessment of different routes for olefins production through the oxidative coupling of methane (OCM): Advances in benchmark technologies, Energy Convers. Manage. 154 (2017) 244–261, http://dx.doi.org/10.1016/j.enconman.2017.10.061.
[6] B.V. Dow Benelux, Personal communication, 2020.
[7] U.S. Department of energy Office of Oil and Natural Gas and Energy, Office of Fossil Energy, Natural gas flaring and venting: State and federal regulatory overview, trends, and impacts, 2019, https://www.energy.gov/sites/prod/files/2019/08/f65/Natural%20Gas%20Flaring%20and%20Venting%20Report.pdf.
[8] M. Ghanta, D. Fahey, B. Subramaniam, Environmental impacts of ethylene production from diverse feedstocks and energy sources, Appl. Petrochem. Res. 4 (2) (2014) 167–179, http://dx.doi.org/10.1007/s13203-013-0029-7.
[9] Market research future: Industry analysis report, business consulting and research, 2020, https://www.marketresearchfuture.com/ accessed at 08-05-2020.
[10] Y. Gambo, A.A. Jalil, S. Triwahyono, A.A. Abdulrasheed, Recent advances and future prospect in catalysts for oxidative coupling of methane to ethylene: A review, J. Ind. Eng. Chem. 59 (2018) 218–229, http://dx.doi.org/10.1016/j.jiec.2017.10.027.
[11] B. Wang, S. Albarracín-Suazo, Y. Pagán-Torres, E. Nikolla, Advances in methane conversion processes, Catal. Today 285 (2017) 147–158, http://dx.doi.org/10.1016/j.cattod.2017.01.023.
[12] M. Scapinello, E. Delikonstantis, G.D. Stefanidis, The panorama of plasma-assisted non-oxidative methane reforming, 2017, http://dx.doi.org/10.1016/j.cep.2017.03.024.
[13] E. Delikonstantis, M. Scapinello, G.D. Stefanidis, Low energy cost conversion of methane to ethylene in a hybrid plasma-catalytic reactor system, Fuel Process. Technol. 176 (2018) 33–42, http://dx.doi.org/10.1016/j.fuproc.2018.03.011.
[14] A. Galadima, O. Muraza, Revisiting the oxidative coupling of methane to ethylene in the golden period of shale gas: A review, 2016, http://dx.doi.org/10.1016/j.jiec.2016.03.027.
[15] L. Fan, Chemical Looping Partial Oxidation: Gasification, Reforming, and Chemical Syntheses, in: Cambridge Series in Chemical Engineering, Cambridge University Press, 2017.
[16] A. Penteado, E. Esche, D. Salerno, H.R. Godini, G. Wozny, Design and assessment of a membrane and absorption based carbon dioxide removal process for oxidative coupling of methane, Ind. Eng. Chem. Res. 55 (27) (2016) 7473–7483, http://dx.doi.org/10.1021/acs.iecr.5b04910.

[17] T.V. Choudhary, E. Aksoylu, D. Wayne Goodman, Nonoxidative activation of methane, Catal. Rev. 45 (1) (2003) 151–203, http://dx.doi.org/10.1081/CR-120017010.
[18] A.I. Olivos-Suarez, À. Szécsényi, E.J. Hensen, J. Ruiz-Martinez, E.A. Pidko, J. Gascon, Strategies for the direct catalytic valorization of methane using heterogeneous catalysis: Challenges and opportunities, ACS Catal. 6 (5) (2016) 2965–2981, http://dx.doi.org/10.1021/acscatal.6b00428.
[19] K. Sun, D.M. Ginosar, T. He, Y. Zhang, M. Fan, R. Chen, Progress in nonoxidative dehydroaromatization of methane in the last 6 years, Ind. Eng. Chem. Res. 57 (6) (2018) 1768–1789, http://dx.doi.org/10.1021/acs.iecr.7b04707.
[20] Y. Xiao, A. Varma, Highly selective nonoxidative coupling of methane over Pt-Bi bimetallic catalysts, ACS Catal. 8 (4) (2018) 2735–2740, http://dx.doi.org/10.1021/acscatal.8b00156.
[21] A.L. Dipu, S. Ohbuchi, Y. Nishikawa, S. Iguchi, H. Ogihara, I. Yamanaka, Direct nonoxidative conversion of methane to higher hydrocarbons over silica-supported nickel phosphide catalyst, ACS Catal. 10 (1) (2020) 375–379, http://dx.doi.org/10.1021/acscatal.9b03955.
[22] X. Guo, G. Fang, G. Li, H. Ma, H. Fan, L. Yu, C. Ma, X. Wu, D. Deng, M. Wei, D. Tan, R. Si, S. Zhang, J. Li, L. Sun, Z. Tang, X. Pan, X. Bao, Direct, nonoxidative conversion of methane to ethylene, aromatics, and hydrogen, Science 344 (6184) (2014) 616–619, http://dx.doi.org/10.1126/science.1253150.
[23] L. Albright, Novel Production Methods for Ethylene, Light Hydrocarbons, and Aromatics, in: Chemical Industries, Taylor & Francis, 1991.
[24] C.-J. Chen, M.H. Back, R.A. Back, Mechanism of the Thermal Decomposition of Methane, 1976, pp. 1–16, http://dx.doi.org/10.1021/bk-1976-0032.ch001.
[25] M. Frenklach, H. Wang, Detailed modeling of soot particle nucleation and growth, Symp. (Int.) Combust. 23 (1) (1991) 1559–1566, http://dx.doi.org/10.1016/S0082-0784(06)80426-1.
[26] W. Sun, A. Hamadi, S. Abid, N. Chaumeix, A. Comandini, An experimental and kinetic modeling study of phenylacetylene decomposition and the reactions with acetylene/ethylene under shock tube pyrolysis conditions, Combust. Flame 220 (2020) 257–271, http://dx.doi.org/10.1016/j.combustflame.2020.06.044.
[27] W. Sun, A. Hamadi, S. Abid, N. Chaumeix, A. Comandini, Probing PAH formation chemical kinetics from benzene and toluene pyrolysis in a single-pulse shock tube, Proc. Combust. Inst. (2020) http://dx.doi.org/10.1016/j.proci.2020.06.077.
[28] O. Kunz, W. Wagner, The GERG-2008 wide-range equation of state for natural gases and other mixtures: An expansion of GERG-2004, J. Chem. Eng. Data 57 (11) (2012) 3032–3091, http://dx.doi.org/10.1021/je300655.
[29] M. Sakbodin, Y. Wu, S.C. Oh, E.D. Wachsman, D. Liu, Hydrogen-permeable tubular membrane reactor: Promoting conversion and product selectivity for non-oxidative activation of methane over an $FeSiO_2$ catalyst, Angew. Chem., Int. Ed. Engl. 55 (52) (2016) 16149–16152, http://dx.doi.org/10.1002/anie.201609991.
[30] Y. Kolbanovskij, V. Shchipachev, N. Chernyak, A. Chernyshova, A. Grigoriev, Impulsnoe Sgatie Gasov v Chimii i Technologii (Pulsed Compression of Gases in Chemistry and Technology), Moskow, Nauka, 1982.
[31] T. Roestenberg, M. Glushenkov, A. Kronberg, H. Krediet, T. vd Meer, Heat transfer study of the pulsed compression reactor, Chem. Eng. Sci. 65 (1) (2010) 88–91, http://dx.doi.org/10.1016/J.CES.2009.01.057.
[32] T. Roestenberg, M. Glushenkov, A. Kronberg, A. Verbeek, T. vd Meer, Experimental study and simulation of syngas generation from methane in the pulsed compression reactor, Fuel 90 (5) (2011) 1875–1883, http://dx.doi.org/10.1016/J.FUEL.2010.11.002.
[33] B. Marcus, Apparatus for chemical production research, US patent 1,586,508, 1926.
[34] B. Atakan, Compression–Expansion processes for chemical energy storage: Thermodynamic optimization for methane, ethane and hydrogen, Energies 12 (17) (2019) 3332, http://dx.doi.org/10.3390/en12173332.
[35] B. Atakan, S.A. Kaiser, J. Herzler, S. Porras, K. Banke, O. Deutschmann, T. Kasper, M. Fikri, R. Schießl, D. Schröder, C. Rudolph, D. Kaczmarek, H. Gossler, S. Drost, V. Bykov, U. Maas, C. Schulz, Flexible energy conversion and storage via high-temperature gas-phase reactions: The piston engine as a polygeneration reactor, Renew. Sustain. Energy Rev. 133 (2020) 110264, http://dx.doi.org/10.1016/j.rser.2020.110264.
[36] C. Rudolph, B. Atakan, Investigation of natural gas/hydrogen mixtures for exergy storage in a piston engine, Energy 218 (2020) 119375, http://dx.doi.org/10.1016/j.energy.2020.119375.
[37] P. Longwell, Chemical Reaction of Methane and of n-Hexane in Ballistic Piston Apparatus (Ph.D. thesis), California Institute of Technology, 1957.
[38] D.A. Kouremenos, X.K. Kakatsios, The three isentropic exponents of dry steam, Eng. Res. 51 (4) (1985) 117–122, http://dx.doi.org/10.1007/BF02558416.
[39] I. Bilousov, M. Bulgakov, V. Savchuk, Modern Marine Internal Combustion Engines, eighth ed., 2020, http://dx.doi.org/10.1007/978-3-030-49749-1.
[40] M.G. Matturro, H.W. Deckman, F. Hershkowitz, A.M. Dean, Rapid thermal pyrolysis of gaseous feeds containing hydrocarbon molecules mixed with an inert working gas, US patent 5,162,599, 1992.
[41] Y. Hidaka, K. Sato, Y. Henmi, H. Tanaka, K. Inami, Shock-tube and modeling study of methane pyrolysis and oxidation, Combust. Flame 118 (3) (1999) 340–358, http://dx.doi.org/10.1016/S0010-2180(99)00010-3.
[42] O. Rokstad, O. Olsvik, A. Holmen, Thermal coupling of methane, Stud. Surf. Sci. Catal. 61 (4) (1991) 533–539, http://dx.doi.org/10.1016/S0167-2991(08)60120-2.
[43] H. Drost, H.D. Klotz, G. Schulz, H.J. Spangenberg, The influence of hydrogen on the kinetics of plasmapyrolytic methane conversion, Plasma Chem. Plasma Process. 5 (1) (1985) 55–65, http://dx.doi.org/10.1007/BF00567909.
[44] F.G. Billaud, F. Baronnet, C.P. Gueret, Thermal coupling of methane in a tubular flow reactor: Parametric study, Ind. Eng. Chem. Res. 32 (8) (1993) 1549–1554, http://dx.doi.org/10.1021/ie00020a003.
[45] J. Moulijn, M. Makkee, A. van Diepen, Chemical Process Technology, Wiley, 2013.
[46] J. Wu, H. Zhang, S. Qin, C. Hu, La-promoted $Na_2WO_4/Mn/SiO_2$ catalysts for the oxidative conversion of methane simultaneously to ethylene and carbon monoxide, Appl. Catal. A: Gen. 323 (2007) 126–134, http://dx.doi.org/10.1016/j.apcata.2007.02.009.